AMERICAN SOCIETY FOR MICROBIOLOGY | Applied and Environmental Microbiology®

GENETICS AND MOLECULAR BIOLOGY

Vibrio fischeri Biofilm Formation Prevented by a Trio of Regulators

Cecilia M. Thompson,[a] Anne E. Marsden,[a] Alice H. Tischler,[a] Jovanka Koo,[b] Karen L. Visick[a]

[a]Department of Microbiology and Immunology, Health Sciences Division, Loyola University Chicago, Maywood, Illinois, USA

[b]Department of Biology, Wheaton College, Wheaton, Illinois, USA

ABSTRACT Biofilms, complex communities of microorganisms surrounded by a self-produced matrix, facilitate attachment and provide protection to bacteria. A natural model used to study biofilm formation is the symbiosis between *Vibrio fischeri* and its host, the Hawaiian bobtail squid, *Euprymna scolopes*. Host-relevant biofilm formation is a tightly regulated process and is observed *in vitro* only with strains that have been genetically manipulated to overexpress or disrupt specific regulators, primarily two-component signaling (TCS) regulators. These regulators control biofilm formation by dictating the production of the symbiosis polysaccharide (Syp-PS), the major component of the biofilm matrix. Control occurs both at and below the level of transcription of the *syp* genes, which are responsible for Syp-PS production. Here, we probed the roles of the two known negative regulators of biofilm formation, BinK and SypE, by generating double mutants. We also mapped and evaluated a point mutation using natural transformation and linkage analysis. We examined traditional biofilm formation phenotypes and established a new assay for evaluating the start of biofilm formation in the form of microscopic aggregates in shaking liquid cultures, in the absence of the known biofilm-inducing signal calcium. We found that wrinkled colony formation is negatively controlled not only by BinK and SypE but also by SypF. SypF is both required for and inhibitory to biofilm formation. Together, these data reveal that these three regulators are sufficient to prevent wild-type *V. fischeri* from forming biofilms under these conditions.

IMPORTANCE Bacterial biofilms promote attachment to a variety of surfaces and protect the constituent bacteria from environmental stresses, including antimicrobials. Understanding the mechanisms by which biofilms form will promote our ability to resolve them when they occur in the context of an infection. In this study, we found that *Vibrio fischeri* tightly controls biofilm formation using three negative regulators; the presence of a single one of these regulators was sufficient to prevent full biofilm development, while disruption of all three permitted robust biofilm formation. This work increases our understanding of the functions of specific regulators and demonstrates the substantial negative control that one benign microbe exerts over biofilm formation, potentially to ensure that it occurs only under the appropriate conditions.

KEYWORDS *Vibrio fischeri*, *binK*, biofilm, response regulator, sensor kinase, *syp*, two-component regulatory systems

Biofilms are complex communities of microorganisms encased in a self-produced matrix that provides protection and permits attachment (1–4). One natural model used to study biofilm formation is the symbiosis between *Vibrio fischeri* and its host, the Hawaiian bobtail squid, *Euprymna scolopes* (5–8). *V. fischeri* colonizes its host by first forming a biofilm on the surface of the symbiotic organ and then dispersing from the

Received 23 May 2018 **Accepted** 12 July 2018

Accepted manuscript posted online 20 July 2018

Citation Thompson CM, Marsden AE, Tischler AH, Koo J, Visick KL. 2018. *Vibrio fischeri* biofilm formation prevented by a trio of regulators. Appl Environ Microbiol 84:e01257-18. https://doi.org/10.1128/AEM.01257-18.

Editor Robert M. Kelly, North Carolina State University

Address correspondence to Karen L. Visick, kvisick@luc.edu.

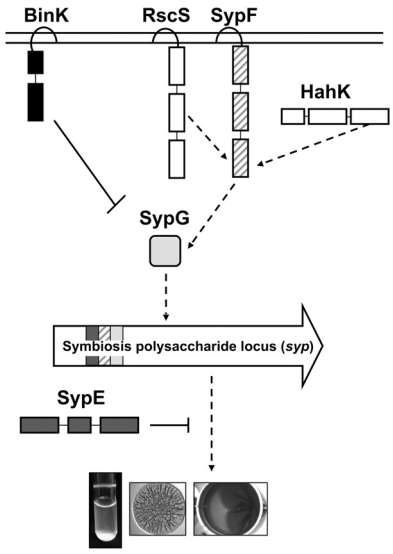

FIG 1 Model of regulation of biofilm formation by *V. fischeri*. In *V. fischeri*, TCS positively and negatively controls biofilm formation by dictating the production of the symbiosis polysaccharide (Syp-PS), the major component of the biofilm matrix. Upon signal activation, RscS initiates a phosphorelay that drives the activation of SypG via SypF's Hpt domain, resulting in increased *syp* transcription and biofilm formation. Recent work demonstrated that HahK also appears to function upstream of the Hpt domain of SypF to promote biofilm formation (11). Two negative regulators, BinK and SypE, also control biofilm formation. The hybrid SK BinK functions as a strong negative regulator of *syp* transcription and biofilm formation (11, 26, 27). SypE inhibits biofilm at a level below transcription via controlling the phosphorylation state of SypA (not shown), whose activity remains unknown (24, 29).

biofilm to enter and colonize the organ (8, 9). Biofilm formation can be observed in laboratory settings by the formation of cohesive wrinkled colonies on solid agar, pellicles at the air-liquid interface in liquid culture under static conditions, and cell clumping in liquid culture under shaking conditions ("shaking cell clumping") (10–12). In contrast to the biofilms that form naturally on the host, the indicated *in vitro* biofilms are formed only by strains that have been genetically manipulated (e.g., by overexpression of positive biofilm regulators and/or disruption of negative regulators). These data suggest that biofilm formation is tightly controlled in *V. fischeri*. At present, seven regulators are known to control biofilm formation. Six of these regulators fall into a large class of regulators known as two-component signaling (TCS) regulators, while the activity of the last regulator remains unknown (Fig. 1).

TCS connects an external signal to a relevant bacterial output using sensor kinases (SKs) that detect the signal and response regulators (RRs) that elicit the response (13). In the simplest pathway, upon signal receipt, the SK autophosphorylates a conserved histidine residue in its HisKA domain. The phosphoryl group is donated to a conserved aspartate residue within the receiver (REC) domain of a partner RR, which then carries out a response, such as binding DNA or altering enzyme activity (14). More complicated pathways exist wherein sequential phosphotransfer events occur on four highly conserved histidine and aspartate residues present in two or more proteins (15). SKs that contain two or more of these four domains are known as hybrid SKs. Extra steps in a phosphorelay are thought to provide opportunities for the cell to exert additional control over the signaling (16–18). Finally, SKs typically have phosphatase activity, permitting them to exert negative control over their cognate RRs (19).

In *V. fischeri*, TCS positively and negatively controls biofilm formation by dictating the production of the symbiosis polysaccharide (Syp-PS), the major component of the biofilm matrix (Fig. 1). Control occurs both at the level of transcription of the 18-gene *syp* locus and at an unknown level below *syp* transcription (8, 12, 20). Mutants defective for TCS regulators exhibit defective or accelerated biofilm formation in culture and, correspondingly, achieve worse or better colonization outcomes during symbiotic colonization (12, 21, 22).

Until recently, investigations of *syp*-dependent biofilm formation relied on the overproduction of positive regulators, such as the overexpression of the hybrid SK RscS or the RR SypG. RscS overexpression induces robust biofilm formation, including wrinkled colonies and pellicles (12), as does the overexpression of SypG in a background that lacks the RR SypE (23, 24). These results led to the model that RscS activates SypG, which directly induces *syp* transcription, and inactivates the inhibitory activity of SypE, culminating in biofilm formation (Fig. 1). In an atypical TCS mechanism, however, the activity of RscS also requires the Hpt domain of SypF, a second hybrid SK with a domain architecture similar to that of RscS (21). Furthermore, another hybrid SK, HahK, appears to similarly feed into the Hpt domain of SypF (11). The absolute requirement for SypF-Hpt in RscS- and HahK-induced biofilm formation brings the total number of known positive regulators to four: RscS, SypG, HahK, and SypF. However, although SypF is considered a positive regulator, the overexpression of wild-type SypF fails to promote biofilm formation; instead, biofilm induction occurs upon the overexpression of SypF1, a variant with increased activity due to a substitution at S247, which is near the putative site of autophosphorylation (H250) (21).

In addition to these four positive regulators, two negative regulators have been identified, SypE and BinK (Fig. 1). Single-copy expression of the RR SypE is sufficient to prevent *V. fischeri* from producing wrinkled colonies when the transcription factor SypG is overexpressed, despite the substantial induction of *syp* transcription that occurs under these conditions (24, 25). The hybrid SK BinK functions as a strong negative regulator of *syp* transcription and biofilm formation (11, 26, 27). *binK* mutants fail to form biofilms under standard laboratory conditions (without the overexpression of a positive regulator). However, recent work revealed that biofilm formation by the *binK* mutant can be induced by the addition of calcium chloride at amounts similar to those found in seawater (28). Specifically, calcium induced the *binK* mutant to produce three *in vitro* biofilm phenotypes: wrinkled colonies, pellicles, and shaking cell clumping (11). In contrast, calcium supplementation is not required when *rscS* is overexpressed: the overexpression of *rscS* is sufficient to induce wrinkled colonies and pellicles (but not shaking cell clumping), even in the absence of calcium. These findings, showing that the loss of BinK does not fully phenocopy RscS overexpression, indicate that other factors are likely involved in negatively controlling biofilm formation in the absence of calcium.

Here, we probed the roles of the two known negative regulators of biofilm formation, BinK and SypE, by generating double mutants and evaluating biofilm formation in the absence of the biofilm-inducing signal calcium. We found that under these conditions, biofilms are negatively controlled not only by BinK and SypE but also by SypF, a known positive regulator. The loss of BinK and SypE, concomitant with a disruption of the inhibitory activity of SypF, permitted *V. fischeri* to form biofilms in the absence of the calcium signal. Together, these data demonstrate that SypF is active as a biofilm inhibitor under standard laboratory conditions and reveal that three regulators prevent biofilm formation by wild-type *V. fischeri*.

RESULTS

Identification of a mutant that forms biofilms in the absence of calcium supplementation. *V. fischeri* encodes two known negative regulators of biofilm formation, the SK BinK (26, 27) and the RR SypE (24, 25, 29). Although some genetically modified strains of *V. fischeri* (e.g., RscS-overexpressing strains [12]) form wrinkled colonies on Luria-Bertani salt (LBS) medium, the standard rich medium used to grow this organism, mutation of neither *binK* nor *sypE* alone permits wrinkled colony formation. We therefore hypothesized that disruption of both negative regulators may be necessary to permit wrinkled colony formation.

To test this hypothesis, we deleted *binK* from strain KV3299, a Δ*sypE* mutant that has been extensively investigated (24, 25, 29), to generate KV7856. Like wild-type strain ES114 (Fig. 2Ai), and as reported previously, the Δ*sypE* mutant formed smooth colonies under these conditions (24, 25, 29) (Fig. 2Aii). Similarly, a strain in which *binK* alone is

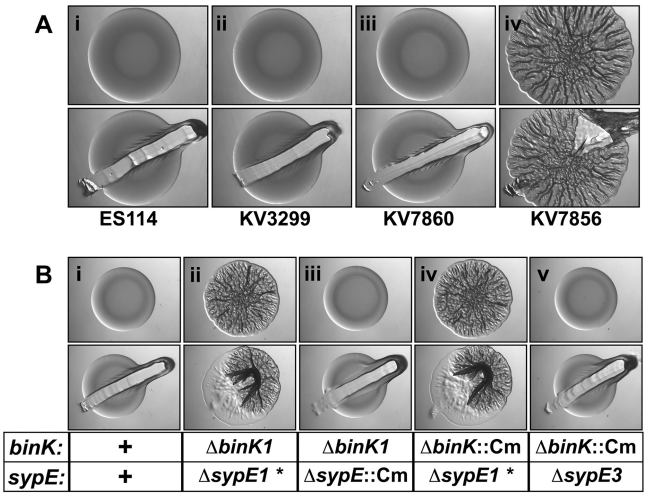

FIG 2 Identification of a mutant that forms wrinkled colonies. (A) Production of wrinkled colonies by the following strains was assessed: the wild type (ES114) (i), Δ*sypE* * (KV3299) (ii), Δ*binK* (KV7860) (iii), and Δ*binK* Δ*sypE* * (KV7856) (iv). Colonies were disrupted to evaluate Syp-PS production. (B) Development of wrinkled colony morphology by three new Δ*binK* Δ*sypE* mutants was assessed at 48 h. The specific *binK* and *sypE* alleles are shown on the bottom along with the hypothesized presence of a putative point mutation (indicated by *), while the corresponding images are shown on the top, for the following strains: the wild type (ES114) (i), Δ*binK1* Δ*sypE1* * (KV7856) (ii), Δ*binK1* Δ*sypE*::FRT-Cm (KV8391) (iii), Δ*binK*::FRT-Cm Δ*sypE1* * (KV8389) (iv), and Δ*binK*::FRT-Cm Δ*sypE3* (KV8390) (v). Colonies were disrupted at 48 h to evaluate Syp-PS production.

deleted (Δ*binK*) formed smooth colonies on LBS medium, as previously reported (11, 26) (Fig. 2Aiii). In contrast, KV7856, defective for the two known negative regulators, produced wrinkled colonies (Fig. 2Aiv). These data initially suggested that BinK and SypE together inhibit biofilm formation.

However, further experimentation indicated that this conclusion was only partially correct: an independently constructed *binK sypE* mutant (Δ*binK1* Δ*sypE*::Cm [where "Cm" represents chloramphenicol]) failed to produce robust wrinkled colonies when grown under the same conditions (Fig. 2Biii) and was, in fact, smooth like the wild-type strain (Fig. 2Bi). To determine the underlying cause of the differing phenotypes, we constructed two additional Δ*binK* Δ*sypE* mutants by introducing a marked *binK* deletion (Δ*binK*::Cm) into two Δ*sypE* deletion mutants, both the original strain KV3299 (Δ*sypE1*) and one that had a distinct derivation (Δ*sypE3*). The former mutant produced wrinkled colonies, similar to the original double mutant (compare Fig. 2Bii and iv), while the latter produced smooth colonies (Fig. 2Bv). Together, these results suggested that disrupting both *binK* and *sypE* was insufficient to generate the wrinkled colony phenotype. As a result, it seemed likely that there was a secondary mutation (indicated by an asterisk) in KV3299, the Δ*sypE* strain used to generate the original double mutant.

To better understand the biofilm-forming capabilities of Δ*binK* Δ*sypE* * mutant strain KV7856, we asked if it similarly exhibited enhanced phenotypes in other biofilm assays, namely, pellicles and shaking cell clumping. Consistent with the observed wrinkled colony phenotypes, KV7856, but not the Δ*sypE* * or Δ*binK* mutants, was competent to form pellicles that developed by 48 h of incubation and were clearly robust within 72 h, as can be observed by the cohesive nature of the pellicle when disrupted (Fig. 3A). In contrast, KV7856 did not differ from the Δ*binK* strain with respect to the shaking cell clumping phenotype: neither strain produced cell clumps when grown with shaking in the absence of calcium, while both strains were competent to do so upon calcium supplementation (see Fig. S1 in the supplemental material). We conclude that additional control mechanisms must be in place to prevent cells from forming large cohesive clumps under shaking conditions in the absence of calcium, and the presence of calcium overrides both this control and negative regulation by SypE and the unknown factor. However, given the other enhanced biofilm phenotypes of KV7856, we

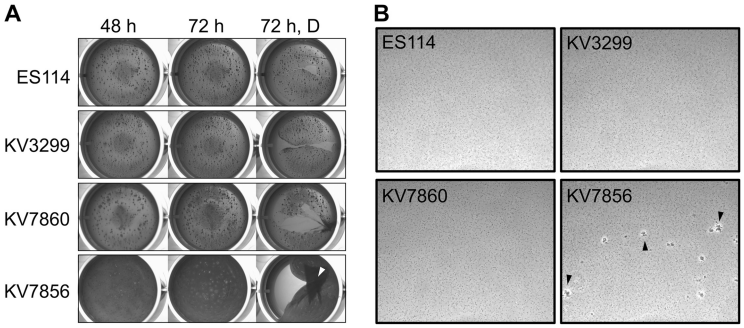

FIG 3 Biofilm formation by the Δ*binK* Δ*sypE* * mutant. (A) Strains were cultured to log phase, standardized in 2 ml LBS medium in a 24-well microtiter plate, and incubated at 24°C. Development of pellicles by the following strains was assessed at the indicated times: the wild type (ES114), Δ*sypE* * (KV3299), Δ*binK* (KV7860), and Δ*binK* Δ*sypE* * (KV7856). At the end of the time course, the pellicles were disrupted with a toothpick to evaluate pellicle strength (72 h, D). Robust pellicle formation is indicated by the white arrow. (B) Microscopic images of aggregates formed in LBS medium without supplemental calcium. Representative images of the following strains were captured at 18 h postinoculation: wild-type ES114, Δ*binK* (KV7860), Δ*sypE* * (KV3299), and Δ*binK* Δ*sypE* * (KV7856). Aggregates are indicated by the black arrows.

revisited the possibility that this strain might exhibit some increase in its capacity to form biofilms when grown without calcium under shaking conditions. We evaluated this possibility using a light microscope to visualize potential biofilm behavior under these conditions. We observed that KV7856, but not the Δ*binK* strain, was able to form microscopic aggregates in the absence of calcium supplementation (Fig. 3B). Furthermore, following overnight growth with shaking, standing cultures of KV7856, but not the controls, became viscous and difficult to pipette (data not shown). Thus, Δ*binK* Δ*sypE* * strain KV7856 produced enhanced biofilms under all tested conditions in the absence of calcium albeit only modestly when grown with shaking.

Identification of a mutation in *sypF*. We next sought to determine the location of the unmarked mutation. We hypothesized that it could be within the large *syp* locus. If so, then it should be possible to observe linkage between the secondary mutation and a representative gene such as *sypE*. Therefore, we introduced chromosomal DNA containing Δ*sypE*::Cm and flanking sequences into the wrinkling-competent strain (Δ*binK* Δ*sypE* *) and selected for Cm^r (Fig. 4A). We expected that if the point mutation were linked to *sypE*, then the incoming sequences would repair the mutation, causing the colonies to become smooth. Indeed, most of the resulting Cm^r colonies were smooth, indicating that the point mutation was closely linked to *sypE*. We obtained a single recombinant, however, that formed a wrinkled colony (Fig. 4A). We hypothesized that in this new strain, KV8265, recombination had occurred such that the point mutation was retained and was now linked to the Cm^r marker.

To more precisely determine the position of the point mutation, we performed additional linkage analyses. Using KV8265 as a template, we amplified Δ*sypE*::Cm and adjacent sequences of different lengths. We introduced these sequences into a recipient strain by natural transformation, selecting for Cm^r. Ultimately, we evaluated the resulting colonies for the ability to wrinkle in the absence of BinK (Fig. 4B); if the mutation was transferred to the recipient, the colonies would become wrinkled. Using this approach, we were able to define the position of the mutation as a region within *sypF* (Fig. 4B). We then sequenced the *sypF* allele from KV8256 to identify the mutation and found that a single nucleotide was deleted from this gene (Fig. 4C); although other changes existed, none resulted in alterations to the predicted protein sequence. The consequence of the nucleotide deletion is a frameshift that would alter the SypF sequence after codon 76 and end the predicted protein after 89 residues; we termed this allele *sypF2*. The mutation was also present in parent strain KV3299 but was absent in the wild-type ES114 strain.

Given the presence of *sypF2* in the well-characterized Δ*sypE* mutant, we wondered if our previous conclusions about SypE function were valid. Specifically, our previous

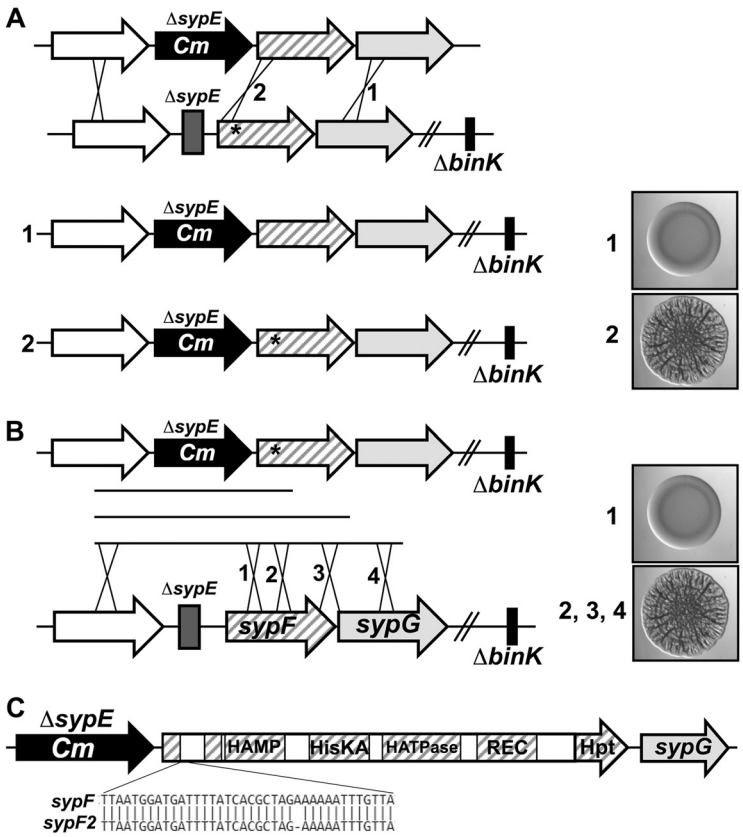

FIG 4 Identification of a mutation in *sypF*. (A) Chromosomal DNAs containing Δ*sypE*::FRT-Cm and flanking sequences were introduced into the wrinkling-competent strain (Δ*binK* Δ*sypE* *) (KV7856) by natural transformation with selection for Cm^r. The resulting colonies were smooth (1) because the incoming DNA repaired the point mutation. There was one exception, a single recombinant that wrinkled, KV8265 (2). Images on the right represent the outcomes but not the actual strains. (B) Using KV8265 as a template, Δ*sypE*::FRT-Cm and adjacent sequences of different lengths were amplified in three separate reactions and introduced into *V. fischeri* by natural transformation and selection for Cm^r. The ability of the resulting Δ*binK* derivatives to form wrinkled colonies was assessed. Images on the right represent the outcomes but not the actual strains. (C) Sequences that were able to confer wrinkling to the Δ*binK* mutant were sequenced, and a mutation was identified in *sypF*. We termed this allele *sypF2*. *sypF2* contained a single nucleotide deletion at nucleotide 227, resulting in a frameshift that ends the predicted protein after residue 89.

work had indicated that SypE was a strong inhibitor of wrinkled colony formation when the response regulator SypG was overexpressed (24, 25), but the presence of the *sypF2* mutation made the role of *sypE* unclear. We therefore compared wrinkled colony formation by *sypG*-overexpressing strain KV3299 as well as two independently constructed Δ*sypE* strains that contain wild-type *sypF*. In contrast to the *sypE*$^+$ control, which formed smooth colonies, all of the *sypE*-defective strains, regardless of the presence of *sypF2*, were competent to form wrinkled colonies (see Fig. S2 in the supplemental material). The presence of *sypF2*, however, substantially accelerated the timing of wrinkled colony formation. Thus, while the *sypF2* allele contributes to the timing of biofilm formation, SypE is, as previously reported, an important negative regulator of wrinkled colony formation.

***sypF2* produces an active protein that promotes biofilms.** Because a frameshift mutation is typically interpreted as a loss-of-function allele, we asked if SypF is dispensable for wrinkled colony formation in the absence of BinK and SypE. In contrast to the wrinkling-competent *sypF2*-containing strain, a *binK* mutant that lacks both *sypE* and *sypF* (Δ*sypEF*) failed to form wrinkled colonies, similar to the Δ*binK* and Δ*binK* Δ*sypE* (*sypF*$^+$) mutants (Fig. 5Ai to iv). In addition, robust wrinkled colony formation could not be restored to the *sypEF* mutant by the reintroduction of the wild-type *sypF* allele (Fig. 5Av). Similarly, while the *binK sypE sypF2* mutant formed robust pellicles, the *binK sypEF* mutant failed to do so, similar to

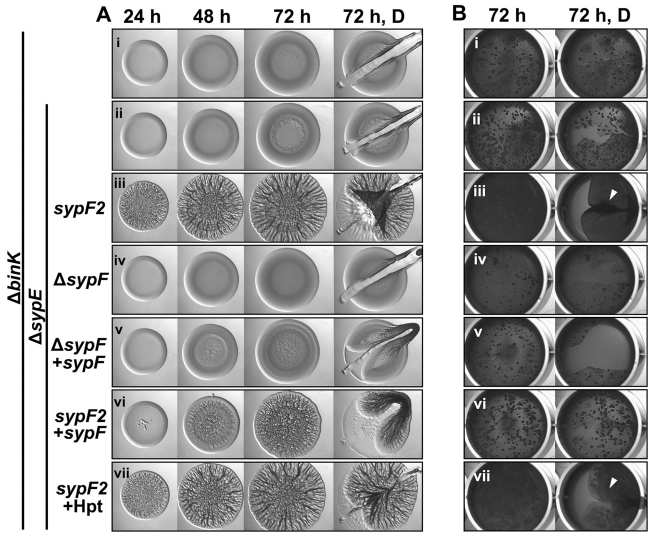

FIG 5 Wrinkled colony formation requires SypF activity. (A) Development of wrinkled colony morphology of the indicated strains was assessed at 24, 48, and 72 h. Colonies were disrupted at the final time point to evaluate Syp-PS production. (B) Strains were cultured to log phase, standardized in 2 ml LBS medium in a 24-well microtiter plate, and incubated at 24°C. Development of pellicles was assessed at 72 h. Robust pellicle formation is indicated by the white arrowheads. For both panels A and B, the following strains were evaluated: Δ*binK* (KV7860) (i), Δ*binK* Δ*sypE* (KV8391) (ii), Δ*binK* Δ*sypE sypF2* (KV7856) (iii), Δ*binK* Δ*sypEF* (KV8055) (iv), Δ*binK* Δ*sypEF att*Tn*7*::*sypF-FLAG* (KV8085) (v), Δ*binK* Δ*sypE sypF2 att*Tn*7*::*sypF-FLAG* (KV8404) (vi), and Δ*binK* Δ*sypE sypF2 att*Tn*7*::*sypF-Hpt-FLAG* (KV8405) (vii).

the *binK* and *binK sypE* (*sypF*$^+$) mutants (Fig. 5B). Pellicle formation with the same timing could not be restored to the Δ*binK* Δ*sypEF* mutant by complementation with *sypF*. All of these strains, except for the uncomplemented Δ*binK* Δ*sypEF* mutant, were competent to produce biofilms when grown with calcium, a result that confirms that the complementing *sypF* allele is functional (see Fig. S3A in the supplemental material). Together, these data suggest that (i) *sypF2* is not a null allele and thus retains some activity necessary for biofilm formation and (ii) wild-type SypF is not a positive regulator in the absence of calcium but, rather, appears to be a negative regulator.

We further tested each of these conclusions. First, if *sypF2* is not a null allele, then we should be able to disrupt its function. Previous work in other genetic contexts has demonstrated that wrinkled colony formation requires the putative site of phosphotransfer, H705, located within the C-terminal histidine phosphotransferase (Hpt) domain of SypF (11, 21). Therefore, we hypothesized that if cells containing *sypF2* retain SypF function, they should also retain the ability to synthesize the Hpt region, including H705. To test the functionality of the C terminus of SypF2, we introduced an H705Q codon mutation into *sypF2*. We found that the H705Q substitution abrogated biofilm formation by the *binK sypE sypF2* strain (Fig. 6Ai to iv and Bi to iv and Fig. S3B). These data support the conclusion that although there is a frameshift mutation in *sypF2*, the Hpt region of SypF must still be produced.

Multiple lines of evidence supported the conclusion that SypF functions as a negative regulator in the absence of calcium. First, we found that an epitope-tagged version of SypF behaved differently from untagged SypF: in contrast to the smooth colonies produced by the Δ*binK* Δ*sypE* (*sypF*$^+$) control, a SypF-hemagglutinin (HA)-expressing derivative produced robust wrinkled colonies with timing similar to that of the *sypF2* (Δ*binK* Δ*sypE sypF2*) strains (Fig. 6Ai to iii, v, and vi). In addition, the expression of SypF-HA in a strain lacking only BinK (*sypE*$^+$) resulted in modest colony architecture albeit after about 48 h of incubation (Fig. 6Avii). These data suggest that the HA tag perturbs the regulatory function of SypF, resulting in an apparent loss of negative function. Similarly, a closer evaluation of the data from the complementation experiment (Fig. 5Av) revealed that SypF-Flag, expressed from a nonnative position in the

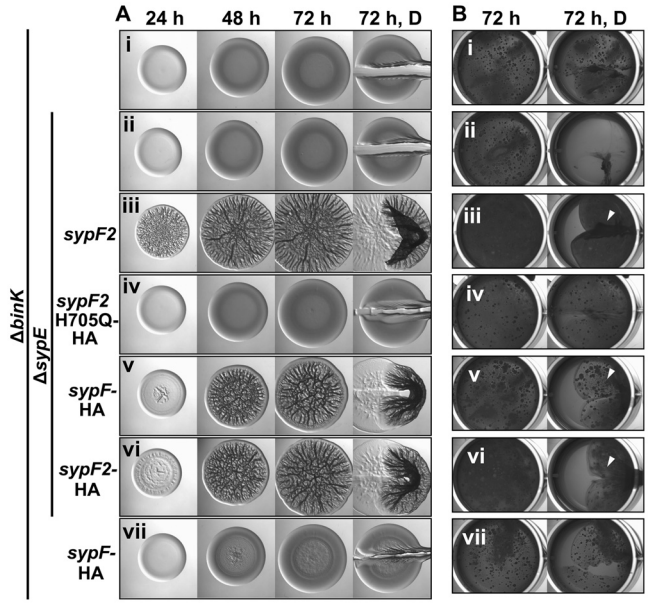

FIG 6 SypF functions as a negative regulator. (A) Development of wrinkled colony morphology of the indicated strains was assessed at 24, 48, and 72 h. (B) Strains were cultured to log phase, standardized in 2 ml LBS medium in a 24-well microtiter plate, and incubated at 24°C. Development of pellicles was assessed at 72 h. Robust pellicle formation is indicated by the white arrowheads. For both panels A and B, the following strains were evaluated: Δ*binK* (KV7860) (i), Δ*binK*::FRT-Cm Δ*sypE* (KV8390) (ii), Δ*binK* Δ*sypE sypF2* (KV7856) (iii), Δ*binK*::FRT-Cm Δ*sypE sypF2-H705Q-HA* (KV8498) (iv), Δ*binK*::FRT Δ*sypE3 sypF-HA* (KV8497) (v), Δ*binK* Δ*sypE sypF2-HA* (KV8499) (vi), and Δ*binK sypF*-HA (KV8467) (vii).

chromosome, failed to restore robust wrinkled colony formation yet permitted the production of colonies with subtle architecture. Because Δ*binK* Δ*sypE* (*sypF*$^+$) double mutant strains form only smooth, noncohesive colonies, these data indicate that the activity of SypF-Flag is also perturbed, diminishing, but not fully disrupting, the negative activity of the protein. Consistent with this conclusion, SypF-Flag exerted a negative effect in the context of SypF2: the introduction of *sypF*-Flag into the *binK sypE sypF2* strain delayed wrinkled colony formation (compare Fig. 5Aiii and vi). In contrast, expression of the isolated Hpt domain alone (SypF-Hpt) did not delay wrinkled colony formation (Fig. 5Avii). Only the Δ*binK* Δ*sypE sypF2* strain expressing SypF-Hpt was competent to promote pellicle formation (Fig. 5Bvi and vii), while both strains were competent to promote shaking cell clumping when grown in calcium (Fig. S3A). These data suggest that wild-type SypF, but not the Hpt domain, displays activity that is inhibitory to biofilm formation in the absence of calcium.

We hypothesized that functional, Hpt-containing SypF protein could be produced from *sypF2* either due to a mechanism like strand slippage, which would permit some full-length protein to be encoded and synthesized, or by the production of a smaller product from a new transcriptional start site. To distinguish between these hypotheses, we attempted to evaluate the production of SypF2-HA by Western blotting. While we could readily detect the SypF-HA control, we were unable to detect SypF2-HA protein even with an excess of protein loaded, despite clear evidence that the C terminus must be functional (Fig. S4). Thus, SypF2-HA may be unstable and/or made in small amounts. In either case, sufficient SypF2 must be made to generate the observed phenotypes. Together, these data indicate that (i) SypF is a required positive regulator of wrinkled colony and pellicle formation in the absence of added calcium, (ii) full-length SypF exhibits inhibitory activity under these conditions, and (iii) SypF2 has positive activity, which wild-type SypF lacks under these conditions, that depends on H705. We propose that the *sypF2* mutation may disconnect the Hpt domain (and other sequences) from the N-terminal transmembrane sensor domain that is predicted to control its activity via a phosphorelay. If this were the case, then the sensor domain of full-length SypF may

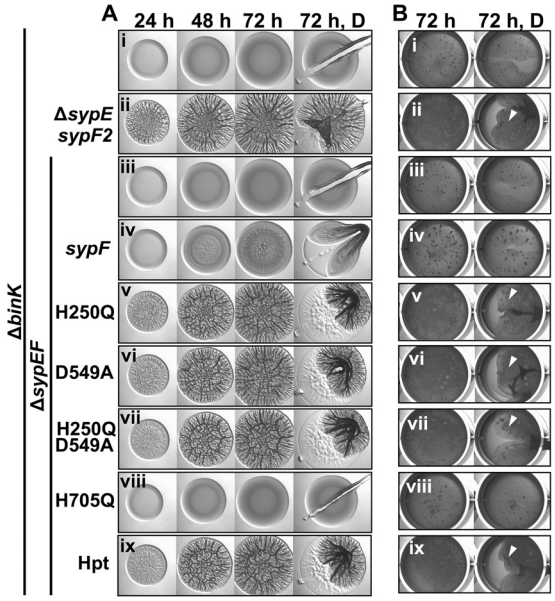

FIG 7 The Hpt domain of SypF promotes biofilm formation. (A) Development of wrinkled colony morphology of the indicated strains was assessed at 24, 48, and 72 h. Colonies were disrupted at the final time point to evaluate Syp-PS production. (B) Strains were cultured to log phase, standardized in 2 ml LBS medium in a 24-well microtiter plate, and incubated at 24°C. Development of pellicles by the indicated strains was assessed at 72 h. At the end of the time course, the pellicles were disrupted with a toothpick to evaluate pellicle strength. Robust pellicle formation is indicated by the white arrow. For both panels A and B, the following strains were evaluated: Δ*binK* (KV7860) (i), Δ*binK* Δ*sypE sypF2* (KV7856) (ii), Δ*binK* Δ*sypE-sypF* (KV8055) (iii), Δ*binK* Δ*sypEF att*Tn*7*::*sypF-FLAG* (KV8085) (iv), Δ*binK* Δ*sypEF att*Tn*7*::*sypF-H250Q-FLAG* (KV8406) (v), Δ*binK* Δ*sypEF att*Tn*7*::*sypF-D549A-FLAG* (KV8088) (vi), Δ*binK* Δ*sypEF att*Tn*7*::*sypF-H250Q-D549A-FLAG* (KV8089) (vii), Δ*binK* Δ*sypEF att*Tn*7*::*sypF-H705Q-FLAG* (KV8087) (viii), and Δ*binK* Δ*sypEF attTn7*::*sypF-Hpt-FLAG* (KV8086) (ix).

function to inhibit wrinkled colony formation under these conditions, potentially by promoting phosphatase activity.

The Hpt domain of SypF promotes wrinkled colony formation. To investigate the mechanism by which SypF controls wrinkled colony formation, we made use of a set of alleles that express SypF variants defective for phosphorelay; we reported previously that only H2 (H705Q), and not H1 (H250Q) or D1 (D549A), is required for biofilm formation (11, 21). We introduced these alleles into the Δ*binK* Δ*sypEF* mutant to see if wrinkled colony formation could be restored. As described above (Fig. 5Av), full-length *sypF* did not promote robust wrinkled colony formation (Fig. 7Ai to iv). However, biofilms readily formed when mutations were introduced outside the Hpt domain, including H1, D1, or H1D1 (H250Q D549A) (Fig. 7Av to vii). In contrast, SypF-H705Q, which contains a mutation within the Hpt domain, failed to promote wrinkled colony formation (Fig. 7Aviii). Importantly, the expression of the C-terminal Hpt domain alone was sufficient to promote biofilm formation by the Δ*binK* Δ*sypEF* mutant, similar to the *sypF2*-expressing Δ*binK* Δ*sypE* mutant (Fig. 7Aix). Similarly, the Hpt domain was sufficient to promote pellicles, but SypF-H705Q could not (Fig. 7Bviii and ix). We conclude that SypF-Hpt is sufficient to promote biofilm formation under a variety of conditions, including with RscS overexpression (11, 21) as well as growth without added calcium. Thus, SypF plays both positive and negative roles in biofilm formation, and the experimental conditions used in this study (e.g., the absence of added calcium) promote the inhibitory activity of SypF. Artificially disconnecting the C-terminal signal transduction machinery from the N-terminal sensory domain removes the negative regulation, promoting biofilm formation.

***sypF2* promotes biofilm formation at the level of transcription.** We hypothesized that if SypF is a negative regulator under these conditions, the transcription of the *syp* locus would be reduced in the presence of wild-type SypF and increased in the

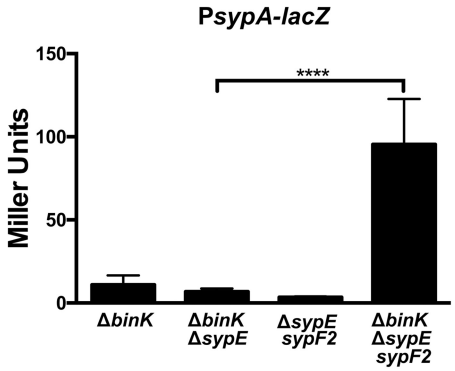

FIG 8 *sypF2* promotes biofilm formation at the level of transcription. Transcription of *syp* was assessed by evaluating the β-galactosidase activity of the indicated strains carrying a *lacZ* reporter fusion to the *sypA* promoter. The following strains were evaluated: Δ*binK* (KV8077), Δ*binK*::FRT Δ*sypE3* (KV8450), Δ*sypE sypF2* (KV8451), and Δ*binK* Δ*sypE sypF2* (KV8454). These strains also contained a deletion of *sypQ*, to prevent complications from biofilm formation. The effects of the *sypF* and *sypF2* alleles on *syp* transcription were evaluated by one-way ANOVA ($P < 0.0001$).

presence of SypF2. We assessed the abilities of these respective alleles to promote *syp* transcription using a *lacZ* reporter. As previously demonstrated, the *binK* mutant exhibited low levels of *syp* transcription in the absence of calcium (11). The *binK* mutant, the Δ*binK* Δ*sypE* (*sypF*$^+$) double mutant, and the Δ*binK* Δ*sypEF* triple mutant all exhibited low levels of *syp* transcription, suggesting that the inhibitory activity of SypF prevents transcription. In contrast, the Δ*binK* Δ*sypE sypF2* strain exhibited a significant ($P < 0.0001$) increase in *syp* transcription compared to the Δ*binK* Δ*sypE* (*sypF*$^+$) double mutant (Fig. 8). Thus, the *sypF2* allele encodes an active, noninhibitory protein competent to induce *syp* transcription.

DISCUSSION

V. fischeri exerts substantial control over biofilm production. Much of the regulation is exerted by two-component regulators, many of which activate transcription of the *syp* locus. Here, we report our findings that a set of three TCS regulators, BinK, SypE, and SypF, prevents wild-type strain ES114 from forming biofilms in a rich medium in the absence of calcium supplementation. We observed roles for these regulators in preventing wrinkled colony development and pellicle formation. In addition, we determined roles for these regulators in inhibiting the start of biofilm formation in liquid culture under shaking conditions by observing microscopic cell aggregation. Together, data from this work reveal that, in addition to substantial positive regulation, *V. fischeri* exerts significant negative regulation over biofilm formation.

Negative regulation by TCS in bacteria is not uncommon. For example, multiple TCS regulators control bioluminescence in *Vibrio harveyi*. At low cell density, three SKs function as kinases to inhibit the production of light by promoting the phosphorylation of the RR LuxO, which in turn indirectly inhibits light production. At high cell density, the three SKs function as phosphatases to dephosphorylate LuxO, inactivating LuxO and allowing light production (30). The loss of a single SK does not prevent cell density-dependent control over bioluminescence. Similarly, the loss of a single negative biofilm regulator in *V. fischeri* does not prevent inhibition of biofilm formation.

BinK and SypE have previously been shown to function as negative regulators (11, 24, 26, 27, 29). The exact function of BinK is not yet known, but BinK negatively impacts biofilm formation via *syp* transcription (11, 26). In contrast, SypE appears to work posttranscriptionally as a serine kinase/phosphatase. While the target of SypE's activity is known, it is unclear how phosphorylation of the target impairs biofilm production. The impact of SypE is also substantial: wild-type cells that overexpress the direct *syp* transcription factor *sypG* fail to form wrinkled colonies in the presence of SypE. Because these two regulators have negative roles, it was reasonable to hypothesize that

together they were sufficient to prevent biofilm formation, and our initial data supported this hypothesis. However, analysis with additional *binK sypE* mutants suggested that the original *sypE* strain, used in numerous studies, carried an additional mutation in *sypF*. We found that this point mutation, while impacting the magnitude of the effect of the *sypE* mutation on wrinkled colony formation, was not responsible for it. Thus, previous work demonstrating the role of SypE as a negative regulator remains valid.

Our ability to map the mutation, and to readily generate multiple additional *binK sypE* double mutants, was possible only due to relatively recent advances in the genetic manipulation of *V. fischeri*. Natural transformation of DNA into *V. fischeri* has been possible since 2010 (31), but the first use of this technology to map mutations was reported in 2015 (32). More recently, tools have been developed to rapidly generate deletions and insertions using PCR-generated DNA (33). Those genetic advances facilitated our studies by supporting the rapid generation of strains with different mutation combinations and/or the addition of an epitope tag to a gene at its native chromosomal location, as well as by permitting us to map unmarked mutations via linkage analysis. These genetic tools, and their new uses in this study, provide a roadmap for future genetic manipulations of *V. fischeri*.

The point mutation in *sypF*, a one-base deletion early in the gene, is predicted to cause a frameshift mutation that should disrupt the function of this gene. Because previous work had demonstrated that SypF plays a vital positive role in biofilm formation, with the C-terminal Hpt domain being necessary and sufficient for SypF function (11, 21), we hypothesized that the point mutation must not prevent the expression of the Hpt domain. While we cannot rule out a role for a truncated N-terminal SypF protein in promoting biofilm formation, several lines of evidence support the conclusion that the SypF2 Hpt domain is made and functional: (i) the Δ*binK* Δ*sypEF* mutant failed to form biofilms, indicating that SypF function is required; (ii) the expression of SypF-Hpt permitted biofilm formation in this background albeit with altered timing; (iii) the Δ*binK* Δ*sypE sypF2* strain, but not the Δ*binK* Δ*sypE* strain, produced high levels of *syp* transcription; and (iv) the activity of SypF2 is lost upon mutation of the *hpt* domain. Furthermore, our results demonstrate that SypF2 not only is functional but also has increased positive activity relative to wild-type SypF. Of particular note is the finding that the expression of SypF delays biofilm formation by the Δ*binK* Δ*sypE sypF2* strain, while the expression of SypF-Hpt does not. These data indicate that full-length SypF exhibits inhibitory activity. Because many sensor kinases also function as phosphatases, it is likely, given our results, that wild-type SypF can function as a phosphatase to inhibit *syp* transcription and biofilm formation. We hypothesize that SypF2 lacks the N-terminal signaling domain and thus contains only downstream signal transduction domains. Such a truncated protein would be separated from the natural control mechanism that, presumably, promotes phosphatase activity, permitting increased activity, as we observed. Thus, we conclude that SypF functions as both a positive and a negative regulator of biofilm formation by *V. fischeri*, with the negative activity dominating under the conditions used here. Although additional work will be necessary to determine what signal(s) controls the activities of SypF, these studies provide conditions under which such a signal(s) can be identified.

Our work included an assessment of a variety of strains that contained active forms of only one or two of the three negative regulators. Single Δ*binK* and double Δ*sypE sypF2* and Δ*binK* Δ*sypE* (*sypF*$^+$) mutants produced smooth colonies, with only the latter strain producing slight colony architecture and stickiness after prolonged growth. While we have yet to generate a Δ*binK sypF2* double mutant, we observed, with some surprise, that a Δ*binK* mutant that expresses HA-tagged SypF produced colonies with subtle three-dimensional (3D) architecture albeit after ~2 days of growth. The additional absence of *sypE* resulted in robust wrinkled colony development. These data suggest that the HA tag perturbs SypF's negative regulatory function to nearly the same extent as the original *sypF2* mutation. Together, these data indicate that all of these negative regulators contribute to preventing wrinkled colony formation, with BinK potentially being the most important.

Consistent with the conclusion that BinK is the most important of the three regulators, we recently reported that calcium supplementation permits a *binK* mutant to form biofilms, including wrinkled colonies on plates, pellicles in static culture, and clumps/rings in shaking cultures; these calcium-induced phenotypes do not require any additional mutations (e.g., *sypE* or *sypF*) (11). The amount of calcium (10 mM) used to induce biofilm formation is physiologically relevant, as it is similar to the amount found in seawater (28), although it remains unclear what influence calcium in seawater has on symbiotic processes. It is also unknown how calcium overcomes the inhibitory activities of SypE and SypF. One simple explanation would be that calcium induces the phosphorylation of SypF (e.g., by activating its kinase activity [11]). SypF would, in turn, inactivate SypE (21, 25). However, calcium can induce biofilm formation by the *binK* mutant that expresses only SypF-Hpt, suggesting that this explanation is not sufficient. An alternative explanation is that other factors are involved. In support of this possibility, we find that the Δ*binK* Δ*sypE sypF2* strain, which proficiently produces wrinkled colonies, fails to form clumps and rings in shaking cultures in the absence of calcium. Similar results have been observed with other biofilm-competent strains (11). Our findings thus identify BinK, SypE, and SypF as negative biofilm regulators in the absence of calcium supplementation and indicate that additional regulation controls shaking cell clumping; whether calcium inactivates the SypE- and/or SypF-dependent negative regulatory mechanisms or bypasses them remains to be determined.

In summary, this work advances our understanding of biofilm control by *V. fischeri* by identifying a set of three negative regulators whose coordinate activities prevent biofilm formation in the absence of added calcium. This study also reports a negative regulatory activity for SypF, a protein whose activity is required for biofilm formation. Together, these findings underscore the importance of biofilm control to *V. fischeri* as well as reveal conditions under which signal transduction processes can be investigated.

MATERIALS AND METHODS

Strains and media. *V. fischeri* strains used in this study are listed in Table 1, and plasmids used are listed in Table 2. *V. fischeri* strains were derived by conjugation or natural transformation. *Escherichia coli* GT115 (InvivoGen, San Diego, CA), π3813 (34), Tam1λpir, Tam1, DH5α, and S17-1λpir were used (35) for cloning and conjugation experiments (36, 37). *V. fischeri* strains were cultured in Luria-Bertani (LB) salt (LBS) medium (38). The following antibiotics were added to LBS medium at the indicated concentrations: chloramphenicol (Cm) at 1 or 2.5 μg ml^{-1}, erythromycin at 2.5 μg ml^{-1}, and tetracycline (Tc) at 2.5 μg ml^{-1}. *E. coli* strains were cultured in LB medium (39) containing 10 g Bacto tryptone, 5 g yeast extract, and 10 g NaCl per liter. The following antibiotics were added to LB medium at the indicated concentrations: kanamycin (Kan) at 50 μg ml^{-1}, Tc at 15 μg ml^{-1}, and ampicillin (Ap) at 100 μg ml^{-1}. For solid media, agar was added to a final concentration of 1.5%.

Bioinformatics. Sequences for *V. fischeri sypF* (VF_A1025) were obtained from the National Center for Biotechnology Information (NCBI) database. Alignments of *sypF* and *sypF2* were generated by using BLAST and the Clustal Omega multiple-sequence alignment program from the EMBL-EBI (http://www.ebi.ac.uk/Tools/msa/clustalw2/) (40–43).

Molecular and genetic techniques. The *binK*, *sypE*, and *sypF* alleles used in this study were generated, and, in some cases, HA epitope tagged, by PCR using primers listed in Table 3. All pARM47-based constructs were inserted into the chromosomal Tn*7* site of *V. fischeri* strains by using tetraparental conjugation (44). *E. coli* strains described above were used for the purposes of cloning, plasmid maintenance, and conjugation. Derivatives of *V. fischeri* were generated via conjugation (45) or by natural transformation (31, 46). PCR SOEing (splicing by overlap extension) (47) reactions were performed by using EMD Millipore Novagen KOD high-fidelity polymerase, and Promega *Taq* was used to confirm gene replacement events. To generate epitope-tagged *sypF*, sequences (~500 bp) upstream and downstream of *sypF* were amplified by PCR and then fused with an HA epitope tag and an Em^r cassette in a PCR SOEing reaction. The final spliced PCR product was introduced into *tfoX*-overexpressing ES114 by natural transformation. The antibiotic resistance marker was used to select for the desired gene replacement mutant, generated by recombination of the PCR product into the chromosome. Chromosomal DNA was isolated from ES114 recombinants by using the DNeasy blood and tissue kit (Qiagen) or the Quick-DNA Microprep kit (Zymogen).

Linkage analysis and sequencing. Linkage of Δ*sypE*::Cm to *sypF2* was assessed through the natural transformation of a Δ*binK* Δ*sypE sypF2* strain using chromosomal Δ*sypE*::Cm DNA, resulting in Δ*binK* Δ*sypE*::Cm *sypF2*, and was confirmed by sequencing. To perform the linkage analysis of *sypF2*, Δ*sypE*::Cm linked to *sypF2* and adjacent sequences of various lengths were amplified. Three reactions were performed in the linkage analysis amplifying Δ*sypE*::Cm and *sypF2*, with 1157 as the forward primer and the following reverse primers: 425, 1221, and 1162. PCR amplification was

TABLE 1 Strains used in this study

Strain	Genotype[a]	Derivation[b]	Reference
ES114	Wild type		36
KV3299	Δ*sypE*		23
KV6439	Δ*sypEF*	Derived from ES114 using pANN17	This study
KV6782	Δ*sypE*	Derived from ES114 using pANN40	This study
KV7410	IG(*yeiR-glmS*)::P*sypA-lacZ att*Tn*7*::Em^r		21
KV7856	Δ*binK* Δ*sypE sypF2*	Derived from KV3299 using pLL2	This study
KV7860	Δ*binK*		11
KV7945	Δ*binK*::FRT-Em Δ*sypE sypF2*	NT KV3299 using PCR DNA generated with primers 2091 and 1268 (ES114), 2097 and 2098 (pKV494), and 2092 and 1271 (ES114)	This study
KV8055	Δ*binK* Δ*sypEF*	Derived from KV6439 using pLL2	This study
KV8077	Δ*binK* Δ*sypQ*::FRT-Cm IG(*yeiR-glmS*)::P*sypA-lacZ att*Tn*7*::Em^r		11
KV8069	Δ*sypQ*::FRT-Cm		11
KV8085	Δ*binK* Δ*sypEF att*Tn*7*::*sypF-FLAG*	Derived from KV8055 using pANN20	This study
KV8086	Δ*binK* Δ*sypEF att*Tn*7*::*sypF-Hpt-FLAG*	Derived from KV8055 using pANN50	This study
KV8087	Δ*binK* Δ*sypEF att*Tn*7*::*sypF-H705Q-FLAG*	Derived from KV8055 using pANN45	This study
KV8088	Δ*binK* Δ*sypEF att*Tn*7*::*sypF-D549A-FLAG*	Derived from KV8055 using pANN21	This study
KV8089	Δ*binK* Δ*sypEF att*Tn*7*::*sypF-H250Q-D549A-FLAG*	Derived from KV8055 using pANN65	This study
KV8124	Δ*binK*::FRT-Cm	NT ES114 using PCR DNA generated with primers 2091 and 1268 (ES114), 2089 and 2090 (pKV495), and 2092 and 1271 (ES114)	This study
KV8151	Δ*sypE*::FRT-Cm	NT ES114 using PCR DNA generated with primers 460 and 2263 (ES114), 2089, and 2090 (pKV495), and 2264 and 425	This study
KV8265	Δ*binK* Δ*sypE*::FRT-Cm *sypF2*	NT KV7856 with chKV8151	This study
KV8389	Δ*binK*::FRT-Cm Δ*sypE sypF2*	NT KV3299 with chKV8124	This study
KV8390	Δ*binK*::FRT-Cm Δ*sypE3*	NT KV6782 with chKV8124	This study
KV8391	Δ*binK* Δ*sypE*::FRT-Cm	NT KV7860 with chKV8151	This study
KV8404	Δ*binK* Δ*sypE sypF2 att*Tn*7*::*sypF-FLAG*	Derived from KV7856 using pANN20	This study
KV8405	Δ*binK* Δ*sypE sypF2 att*Tn*7*::*sypF-Hpt-FLAG*	Derived from KV7856 using pANN50	This study
KV8406	Δ*binK* Δ*sypEF att*Tn*7*::*sypF-H250Q-FLAG*	Derived from KV8055 using pANN45	This study
KV8419	Δ*binK*::FRT Δ*sypE3* IG(*yeiR-glmS*)::P*sypA-lacZ att*Tn*7*::Em^r	NT KV8512 with chKV7410	This study
KV8420	Δ*sypE sypF2* IG(*yeiR-glmS*)::P*sypA-lacZ att*Tn*7*::Em^r	NT KV3299 with chKV7410	This study
KV8450	Δ*binK*::FRT Δ*sypE3* Δ*sypQ*::FRT-Cm IG(*yeiR-glmS*)::P*sypA-lacZ att*Tn*7*::Em^r	NT KV8419 with chKV8069	This study
KV8454	Δ*binK* Δ*sypE sypF2* Δ*sypQ*::FRT-Cm IG(*yeiR-glmS*)::P*sypA-lacZ att*Tn*7*::Em^r	NT KV7856 with chKV8069, followed by NT with chKV7410	This study
KV8467	Δ*binK sypF-HA* IG(*sypF-sypG*)::Em^r	NT KV7860 with chKV8497	This study
KV8469	Δ*binK*::FRT-Em Δ*sypE*::FRT-Cm	NT KV7945 using PCR DNA generated with primers 1157 and 425 (KV8265)	This study
KV8470	Δ*binK*::FRT-Em Δ*sypE*::FRT-Cm *sypF2*	NT KV7945 using PCR DNA generated with primers 1157 and 425 (KV8265)	This study
KV8497	Δ*binK*::FRT Δ*sypE3 sypF-HA* IG(*sypF-sypG*)::Em^r	NT KV8512 using PCR DNA generated with primers 1223 and 2348 (ES114), 2089 and 2090 (pKV494), and 2362 and 271 (ES114)	This study
KV8498	Δ*binK*::FRT-Cm Δ*sypE sypF2-H705Q-HA* IG(*sypF-sypG*)::Em^r	NT KV3299 using PCR DNA generated with primers 1223 and 1793 (KV8497) and primers 1794 and 271 (KV8497), followed by NT with chKV8124	This study
KV8499	Δ*binK* Δ*sypE sypF2-HA* IG(*sypF-sypG*)::Em^r	NT KV7856 with chKV8467	This study
KV8512	Δ*binK*::FRT Δ*sypE3*	Removal of Cm cassette from KV8390 with Flp (pKV496)	This study

[a]IG, intergenic.

[b]Derivation of strains constructed in this study. NT, natural transformation of a pLostfoX- or pLostfoX-Kan-carrying version of the strain with the indicated chromosomal (ch) DNA or with a PCR SOEing product generated by using the indicated primers and templates (in parentheses).

TABLE 2 Plasmids used in this study

Plasmid	Description[a]	Reference or source
pANN17	Derivative of pKV363 + sequences flanking *sypEF*	21
pANN20	pEVS107 + P*lac-sypF-FLAG*	21
pANN21	pEVS107 + P*lac-sypF-D549A-FLAG*	21
pANN24	pEVS107 + P*lac-sypF-H250Q-FLAG*	21
pANN32	pKV363 + sequences flanking *sypE* and *sypF*, generated with primers 1219 and 519 and primers 1249 and 1375	This study
pANN40	pKV363 + sequences flanking *sypE*, generated with primers 1219 and 519 and primers 1220 and 684	This study
pANN45	pEVS107 + P*lac-sypF-H705Q-FLAG*	21
pANN50	pEVS107 + P*lac-sypF-Hpt-FLAG*	21
pANN65	pEVS107 + P*lac-sypF-H250Q-D549A-FLAG*	21
pCLD56	pKV282 + *sypG*	24
pEVS104	Conjugal plasmid	50
pEVS107	Tn*7* delivery plasmid; Em^r Km^r	44
pEVS170	Vector containing Em^r Km^r	51
pJET	Commercial cloning vector; Ap^r	Thermo Fisher
pKV282	Low-copy-no. vector; Tc^r	25
pKV363	Suicide plasmid	37
pKV494	pJET + FRT-Em^r	33
pKV495	pJET + FRT-Cm^r	33
pKV496	pJET + Flp recombinase	33
pLL2	pKV363 + sequences flanking *binK*	11
pLosTfoX	Expresses TfoX; Cm^r	31
pLostfoX-Kan	Expresses TfoX; Km^r	46
pUX-BF13	Tn*7* transposase-expressing vector	52

[a]Details on construction are included for plasmids generated in this study; ES114 was used as a template for PCRs.

performed by using EMD Millipore Novagen KOD high-fidelity polymerase or Invitrogen AccuPrime high-fidelity *Taq* polymerase. The final PCR product was introduced into the *tfoX*-overexpressing Δ*binK* strain by natural transformation. The antibiotic resistance marker was used to select for the desired gene replacement mutant, generated by recombination of the PCR product into the chromosome. Because the *tfoX*-overexpressing Δ*binK* mutant exhibited decreased transformation efficiency relative to the wild type, in some cases the PCR products were first introduced into ES114, followed by the introduction of a marked Δ*binK* allele into multiple original colonies. Specifically, for the recombination events indicated in Fig. 4B (sequences 1 and 2), KV8265 was used as a template for PCR with primers 1157 and 425 (template KV8265) and then used to transform ES114. Seven colonies that maintained the *tfoX* plasmid were isolated on medium containing Cm and Km and used as a recipient for transformation with chromosomal DNA from KV7945 (Δ*binK*::Tm^r). One of these (KV8470) formed wrinkled colonies, while the remainder (represented by KV8469) formed smooth colonies. *sypF* alleles were sequenced by first amplifying *sypF* sequences, followed by column purifying the resulting PCR products, which were then sequenced by using primer 425 and, for KV8265, primer 684, 1223, or 2264. KV3299, KV8265, KV8469, and KV8498 contained the frameshift mutation of *sypF2*, while ES114 and KV8470 contained the wild-type *sypF* sequence in this region. Sequencing reactions were performed by ACGT, Inc. (Wheeling, IL).

Wrinkled colony formation assay. To observe wrinkled colony formation, the indicated *V. fischeri* strains were streaked onto LBS agar plates. Single colonies were then cultured with shaking in 5 ml LBS broth overnight at 28°C. The strains were then subcultured the following day in 5 ml of fresh medium. Following growth to early log phase, the cultures were standardized to an optical density at 600 nm (OD_{600}) of 0.2 by using LBS medium. Ten microliters of diluted cultures was spotted onto LBS agar plates and grown at 24°C. Images of the spotted cultures were acquired over the course of wrinkled colony formation at the indicated times by using a Zeiss Stemi 2000-C dissecting microscope and a Jenoptik Progres Gryphax series Subra camera. At the end of the time course, the colonies were disrupted with a toothpick to assess colony cohesiveness, which is an indicator of symbiosis polysaccharide (Syp-PS) production (48).

Pellicle formation assay. To assess pellicle formation, *V. fischeri* strains were grown overnight and subcultured with shaking as described above. Following growth to mid-log phase, the cultures were standardized to an OD_{600} of 0.2 using LBS medium in a 24-well microtiter plate. Inoculated microtiter plates were incubated statically at 24°C. Images of the microtiter wells were acquired over the course of pellicle formation at the indicated times by using a Zeiss Stemi 2000-C dissecting microscope and a Jenoptik Progres Gryphax series Subra camera. At the end of the time course, the pellicles were disrupted with a toothpick to assess pellicle strength.

Microscopic aggregation assay. Differential interference contrast (DIC) images of strains grown without calcium were assessed for aggregation by using an Optronics MagnaFire S60800 charge-coupled-device (CCD) microscope camera attached to a Leica DM IRB with a Prior Lumen 200 light source. Images were taken at a ×200 magnification (20× objective lens and 10× eyepiece).

β-Galactosidase assay. Strains carrying a *lacZ* reporter fusion to the *sypA* promoter were grown in triplicate at 24°C in LBS medium. Strains were subcultured in 20 ml of fresh medium in 125-ml baffled

TABLE 3 Primers

Primer	Sequence (5′–3′)[a]
271	CTCGGCGCATACTTCTTTAC
425	AGGGGTTCGTATTTCGTGACTC
460	GCCTTGATAGGAGCATTATAATG
519	GGGTGGTGTTACTCGCTAC
683	aagctagcCAATAAAAAGCAAACATTGCAA
684	ACTCGCATCGGTGTCAGC
1157	catactaagtgcggccgcctaGCCTTGATAGGAGCATTATAATGAG
1162	taggcggccgcacttagtatgTCCAAAATTACGGCTATCAAGCAG
1219	taggcggccgcacttagtatgTGTGGGCTTTGTATCTGAAAAAAG
1220	catactaagtgcggccgcctaCTGTTAATTGAGATTCAATAAAAAG
1221	taggcggccgcacttagtatgGTCTTCGACTAATAATACTTTCTG
1223	GAATGTCTTGCTAAGTACCTG
1249	catactaagtgcggccgcctaAAACAAGGTTTCTCAAAATAAAAG
1268	ggagccaacagcaagactta
1271	TGCCACCGTTTCTCGTGTAG
1375	TCATCATTCCGATTCTTCATAG
1793	AATGCACTGCTTCCTAATGTTTGCGCTTCAAACTC
1794	ATGCATTAGAGTTTGAAGCGCAAACATTAGGAAGC
2089	CCATACTTAGTGCGGCCGCCTA
2090	CCATGGCCTTCTAGGCCTATCC
2091	taggcggccgcactaagtatggATAGCAAGCTAACGCGAGAATGC
2092	ggataggcctagaaggccatggTTGGAAGCGTATACATAAATAATGATTC
2097	ccatacttagtgcggccgcctagaagttcctattctctagaaagtataggaacttcggatccTAAGAGTGTGTTGATAGTGCAG
2098	ccatggccttctaggcctatccgaagttcctatactttctagagaataggaacttcGGATCCTTATTTCCTCCCGTTAAATAATAG
2263	taggcggccgcactaagtatggATTCATGATTACACCACTGTTG
2264	ggataggcctagaaggccatggCCCAATGACGATGCATTATTGC
2348	taggcggccgcactaagtatggaTTATGCATAATCTGGAACATCATATGGATAttttgagaaaccttgtttatttc
2362	ggataggcctagaaggccatggAAGAATAAAACAAAATTCGCTAGG

[a]Lowercase type indicates "tails" added to the PCR product that were not complementary to the target DNA.

flasks, the OD_{600} was measured, and samples (1 ml) were collected after 22 h of growth. Cells were resuspended in Z-buffer and lysed with chloroform. The β-galactosidase activity of each sample was assayed as described previously (49) and measured by using a Synergy H1 microplate reader (BioTek). The assay was performed at least three independent times. Statistical analysis was performed by using one-way analysis of variance (ANOVA).

SUPPLEMENTAL MATERIAL

Supplemental material for this article may be found at https://doi.org/10.1128/AEM.01257-18.

SUPPLEMENTAL FILE 1, PDF file, 0.5 MB.

ACKNOWLEDGMENTS

We thank Valerie Ray, Louise Lie, and Allison Norsworthy for strain construction and members of the laboratory for thoughtful discussions and review of the manuscript.

This work was supported by NIH grant R01 GM114288 awarded to K.L.V. and by the Wheaton College Aldeen Grant awarded to J.K.

REFERENCES

1. Donlan RM. 2001. Biofilms and device-associated infections. Emerg Infect Dis 7:277–281. https://doi.org/10.3201/eid0702.010226.
2. Flemming HC, Neu TR, Wozniak DJ. 2007. The EPS matrix: the "house of biofilm cells." J Bacteriol 189:7945–7947. https://doi.org/10.1128/JB.00858-07.
3. Flemming HC, Wingender J. 2010. The biofilm matrix. Nat Rev Microbiol 8:623–633. https://doi.org/10.1038/nrmicro2415.
4. O'Toole G, Kaplan HB, Kolter R. 2000. Biofilm formation as microbial development. Annu Rev Microbiol 54:49–79. https://doi.org/10.1146/annurev.micro.54.1.49.
5. McFall-Ngai M. 2014. Divining the essence of symbiosis: insights from the squid-vibrio model. PLoS Biol 12:e1001783. https://doi.org/10.1371/journal.pbio.1001783.
6. McFall-Ngai MJ. 2014. The importance of microbes in animal development: lessons from the squid-vibrio symbiosis. Annu Rev Microbiol 68:177–194. https://doi.org/10.1146/annurev-micro-091313-103654.
7. Stabb E, Visick K. 2013. *Vibrio fischeri*: a bioluminescent light-organ symbiont of the bobtail squid *Euprymna scolopes*, p 497–532. *In* Rosenberg E, DeLong EF, Lory S, Stackebrandt E, Thompson F (ed), The prokaryotes, 4th ed. Springer, New York, NY.
8. Visick KL. 2009. An intricate network of regulators controls biofilm formation and colonization by Vibrio fischeri. Mol Microbiol 74:782–789. https://doi.org/10.1111/j.1365-2958.2009.06899.x.
9. Nyholm SV, Stabb EV, Ruby EG, McFall-Ngai MJ. 2000. Establishment of an animal-bacterial association: recruiting symbiotic vibrios from the environment. Proc Natl Acad Sci U S A 97:10231–10235. https://doi.org/10.1073/pnas.97.18.10231.
10. Darnell CL, Hussa EA, Visick KL. 2008. The putative hybrid sensor kinase

SypF coordinates biofilm formation in Vibrio fischeri by acting upstream of two response regulators, SypG and VpsR. J Bacteriol 190:4941–4950. https://doi.org/10.1128/JB.00197-08.
11. Tischler AH, Lie L, Thompson CM, Visick KL. 2018. Discovery of calcium as a biofilm-promoting signal for *Vibrio fischeri* reveals new phenotypes and underlying regulatory complexity. J Bacteriol 200:e00016-18. https://doi.org/10.1128/JB.00016-18.
12. Yip ES, Geszvain K, DeLoney-Marino CR, Visick KL. 2006. The symbiosis regulator *rscS* controls the *syp* gene locus, biofilm formation and symbiotic aggregation by *Vibrio fischeri*. Mol Microbiol 62:1586–1600. https://doi.org/10.1111/j.1365-2958.2006.05475.x.
13. Stock AM, Robinson VL, Goudreau PN. 2000. Two-component signal transduction. Annu Rev Biochem 69:183–215. https://doi.org/10.1146/annurev.biochem.69.1.183.
14. Galperin MY. 2010. Diversity of structure and function of response regulator output domains. Curr Opin Microbiol 13:150–159. https://doi.org/10.1016/j.mib.2010.01.005.
15. Wuichet K, Cantwell BJ, Zhulin IB. 2010. Evolution and phyletic distribution of two-component signal transduction systems. Curr Opin Microbiol 13:219–225. https://doi.org/10.1016/j.mib.2009.12.011.
16. Jung K, Fried L, Behr S, Heermann R. 2012. Histidine kinases and response regulators in networks. Curr Opin Microbiol 15:118–124. https://doi.org/10.1016/j.mib.2011.11.009.
17. Uhl MA, Miller JF. 1996. Integration of multiple domains in a two-component sensor protein: the Bordetella pertussis BvgAS phosphorelay. EMBO J 15:1028–1036.
18. West AH, Stock AM. 2001. Histidine kinases and response regulator proteins in two-component signaling systems. Trends Biochem Sci 26:369–376. https://doi.org/10.1016/S0968-0004(01)01852-7.
19. Kenney LJ. 2010. How important is the phosphatase activity of sensor kinases? Curr Opin Microbiol 13:168–176. https://doi.org/10.1016/j.mib.2010.01.013.
20. Shibata S, Yip ES, Quirke KP, Ondrey JM, Visick KL. 2012. Roles of the structural symbiosis polysaccharide (syp) genes in host colonization, biofilm formation, and polysaccharide biosynthesis in Vibrio fischeri. J Bacteriol 194:6736–6747. https://doi.org/10.1128/JB.00707-12.
21. Norsworthy AN, Visick KL. 2015. Signaling between two interacting sensor kinases promotes biofilms and colonization by a bacterial symbiont. Mol Microbiol 96:233–248. https://doi.org/10.1111/mmi.12932.
22. Yip ES, Grublesky BT, Hussa EA, Visick KL. 2005. A novel, conserved cluster of genes promotes symbiotic colonization and sigma-dependent biofilm formation by *Vibrio fischeri*. Mol Microbiol 57:1485–1498. https://doi.org/10.1111/j.1365-2958.2005.04784.x.
23. Hussa EA, Darnell CL, Visick KL. 2008. RscS functions upstream of SypG to control the syp locus and biofilm formation in Vibrio fischeri. J Bacteriol 190:4576–4583. https://doi.org/10.1128/JB.00130-08.
24. Morris AR, Visick KL. 2013. Inhibition of SypG-induced biofilms and host colonization by the negative regulator SypE in *Vibrio fischeri*. PLoS One 8:e60076. https://doi.org/10.1371/journal.pone.0060076.
25. Morris AR, Darnell CL, Visick KL. 2011. Inactivation of a novel response regulator is necessary for biofilm formation and host colonization by Vibrio fischeri. Mol Microbiol 82:114–130. https://doi.org/10.1111/j.1365-2958.2011.07800.x.
26. Brooks JF, II, Mandel MJ. 2016. The histidine kinase BinK is a negative regulator of biofilm formation and squid colonization. J Bacteriol 198:2596–2607. https://doi.org/10.1128/JB.00037-16.
27. Pankey SM, Foxall RL, Ster IM, Perry LA, Schuster BM, Donner RA, Coyle M, Cooper VS, Whistler CA. 2017. Host-selected mutations converging on a global regulator drive an adaptive leap towards symbiosis in bacteria. Elife 6:e24414. https://doi.org/10.7554/eLife.24414.
28. Pilson MEQ. 1998. An introduction to the chemistry of the sea. Prentice Hall, Upper Saddle River, NJ.
29. Morris AR, Visick KL. 2013. The response regulator SypE controls biofilm formation and colonization through phosphorylation of the syp-encoded regulator SypA in Vibrio fischeri. Mol Microbiol 87:509–525. https://doi.org/10.1111/mmi.12109.
30. Ng WL, Bassler BL. 2009. Bacterial quorum-sensing network architectures. Annu Rev Genet 43:197–222. https://doi.org/10.1146/annurev-genet-102108-134304.
31. Pollack-Berti A, Wollenberg MS, Ruby EG. 2010. Natural transformation of Vibrio fischeri requires tfoX and tfoY. Environ Microbiol 12:2302–2311. https://doi.org/10.1111/j.1462-2920.2010.02250.x.
32. Brooks JF, II, Gyllborg MC, Kocher AA, Markey LE, Mandel MJ. 2015. TfoX-based genetic mapping identifies Vibrio fischeri strain-level differences and reveals a common lineage of laboratory strains. J Bacteriol 197:1065–1074. https://doi.org/10.1128/JB.02347-14.
33. Visick KL, Hodge-Hanson KM, Tischler AH, Bennett AK, Mastrodomenico V. 2018. Tools for rapid genetic engineering of *Vibrio fischeri*. Appl Environ Microbiol 84:e00850-18. https://doi.org/10.1128/AEM.00850-18.
34. Le Roux F, Binesse J, Saulnier D, Mazel D. 2007. Construction of a Vibrio splendidus mutant lacking the metalloprotease gene vsm by use of a novel counterselectable suicide vector. Appl Environ Microbiol 73:777–784. https://doi.org/10.1128/AEM.02147-06.
35. Simon R, Priefer U, Pühler A. 1983. A broad host range mobilization system for in vivo genetic engineering: transposon mutagenesis in Gram negative bacteria. Biotechnology 1:784–791. https://doi.org/10.1038/nbt1183-784.
36. Boettcher KJ, Ruby EG. 1990. Depressed light emission by symbiotic Vibrio fischeri of the sepiolid squid Euprymna scolopes. J Bacteriol 172:3701–3706. https://doi.org/10.1128/jb.172.7.3701-3706.1990.
37. Visick KL, Skoufos LM. 2001. Two-component sensor required for normal symbiotic colonization of Euprymna scolopes by Vibrio fischeri. J Bacteriol 183:835–842. https://doi.org/10.1128/JB.183.3.835-842.2001.
38. Stabb EV, Reich KA, Ruby EG. 2001. Vibrio fischeri genes hvnA and hvnB encode secreted NAD(+)-glycohydrolases. J Bacteriol 183:309–317. https://doi.org/10.1128/JB.183.1.309-317.2001.
39. Davis RW. 1980. Advanced bacterial genetics: a manual for genetic engineering. Cold Spring Harbor Laboratory, Cold Spring Harbor, NY.
40. Altschul SF, Madden TL, Schäffer AA, Zhang J, Zhang Z, Miller W, Lipman DJ. 1997. Gapped BLAST and PSI-BLAST: a new generation of protein database search programs. Nucleic Acids Res 25:3389–3402. https://doi.org/10.1093/nar/25.17.3389.
41. Altschul SF, Wootton JC, Gertz EM, Agarwala R, Morgulis A, Schäffer AA, Yu YK. 2005. Protein database searches using compositionally adjusted substitution matrices. FEBS J 272:5101–5109. https://doi.org/10.1111/j.1742-4658.2005.04945.x.
42. Larkin MA, Blackshields G, Brown NP, Chenna R, McGettigan PA, McWilliam H, Valentin F, Wallace IM, Wilm A, Lopez R, Thompson JD, Gibson TJ, Higgins DG. 2007. Clustal W and Clustal X version 2.0. Bioinformatics 23:2947–2948. https://doi.org/10.1093/bioinformatics/btm404.
43. Sievers F, Wilm A, Dineen D, Gibson TJ, Karplus K, Li W, Lopez R, McWilliam H, Remmert M, Söding J, Thompson JD, Higgins DG. 2011. Fast, scalable generation of high-quality protein multiple sequence alignments using Clustal Omega. Mol Syst Biol 7:539. https://doi.org/10.1038/msb.2011.75.
44. McCann J, Stabb EV, Millikan DS, Ruby EG. 2003. Population dynamics of *Vibrio fischeri* during infection of *Euprymna scolopes*. Appl Environ Microbiol 69:5928–5934. https://doi.org/10.1128/AEM.69.10.5928-5934.2003.
45. DeLoney CR, Bartley TM, Visick KL. 2002. Role for phosphoglucomutase in Vibrio fischeri-Euprymna scolopes symbiosis. J Bacteriol 184:5121–5129. https://doi.org/10.1128/JB.184.18.5121-5129.2002.
46. Brooks JF, II, Gyllborg MC, Cronin DC, Quillin SJ, Mallama CA, Foxall R, Whistler C, Goodman AL, Mandel MJ. 2014. Global discovery of colonization determinants in the squid symbiont *Vibrio fischeri*. Proc Natl Acad Sci U S A 111:17284–17289. https://doi.org/10.1073/pnas.1415957111.
47. Ho SN, Hunt HD, Horton RM, Pullen JK, Pease LR. 1989. Site-directed mutagenesis by overlap extension using the polymerase chain reaction. Gene 77:51–59. https://doi.org/10.1016/0378-1119(89)90358-2.
48. Ray VA, Driks A, Visick KL. 2015. Identification of a novel matrix protein that promotes biofilm maturation in Vibrio fischeri. J Bacteriol 197:518–528. https://doi.org/10.1128/JB.02292-14.
49. Miller JH. 1972. Experiments in molecular genetics. Cold Spring Harbor Laboratory, Cold Spring Harbor, NY.
50. Stabb EV, Ruby EG. 2002. RP4-based plasmids for conjugation between Escherichia coli and members of the Vibrionaceae. Methods Enzymol 358:413–426. https://doi.org/10.1016/S0076-6879(02)58106-4.
51. Lyell NL, Dunn AK, Bose JL, Vescovi SL, Stabb EV. 2008. Effective mutagenesis of *Vibrio fischeri* by using hyperactive mini-Tn*5* derivatives. Appl Environ Microbiol 74:7059–7063. https://doi.org/10.1128/AEM.01330-08.
52. Bao Y, Lies DP, Fu H, Roberts GP. 1991. An improved Tn7-based system for the single-copy insertion of cloned genes into chromosomes of gram-negative bacteria. Gene 109:167–168. https://doi.org/10.1016/0378-1119(91)90604-A.